ELSEVIER

Chemical Engineering Journal 85 (2002) 369–378

Chemical Engineering Journal

www.elsevier.com/locate/cej

Short communication

Determination of a coalescence parameter from batch-settling experiments

Martin Henschke, Lars Holger Schlieper, Andreas Pfennig*

Lehrstuhl für Thermische Verfahrenstechnik, RWTH Aachen, Wüllnerstr. 5, D-52056 Aachen, Germany

Received 6 June 2001; received in revised form 10 October 2001; accepted 15 October 2001

Abstract

Until today, neither measurements nor theory are able to describe the complex processes at the interface that occur during coalescence in liquid–liquid dispersions in a detailed way. With the model presented in this study, it is possible to characterize coalescence processes with a single integral coalescence parameter. This parameter is obtained from a simple batch-settling experiment. If experimental data are evaluated based on this model, it is ensured that the parameter is independent of the experimental equipment, mixing intensity and volume fraction of the dispersed phase. Furthermore, the drop size in the dense-packed zone can be determined with this model.

Keywords: Coalescence; Film drainage; Liquid–liquid dispersion; Batch-settling experiment

1. Introduction

In several chemical engineering processes, e.g. azeotropic distillation, liquid–liquid extraction and liquid–membrane permeation, mixtures have to be handled which consist of two saturated liquid phases with one phase (dispersed phase) being dispersed within the other phase (continuous phase) in the form of small drops. Such a mixture is called liquid–liquid dispersion. A liquid–liquid dispersion can easily be obtained by filling a cylindrical bottle with two liquids—usually an organic and an aqueous phase—and by subsequently shaking it vigorously. As a result, the aqueous phase will be dispersed within the organic phase or vice versa depending on the volume ratio between the two phases.

In Fig. 1, the decay of a dispersion in a batch-settling experiment is shown. In this example, the heavy phase is dispersed. After the shaking is stopped (time $t = 0$), the sedimentation of the droplets directed towards their continuous phase can be observed. If drop sedimentation is faster than drop–interface coalescence (drops combining with their corresponding continuous phase), the droplets will accumulate in a dense-packed zone. Within this zone, the droplets grow in size due to drop–drop coalescence. Thus drops eventually coalescing at the interface are larger than the drops originally generated. After a certain time ($t = t_E$), all drops have vanished and a distinct interface can be observed inside the cylinder.

Trace impurities present one problem in modeling phase separation in the batch-settling experiment as well as in steady-state operated technical settlers. These impurities cannot be avoided in practice and they change the settling behavior significantly without measurably changing the physical properties ($\Delta\rho$, η_c, η_d, σ) of the compounds which are usually regarded to be responsible for phase separation [1–4]. Effects like interfacial mobility and van der Waals attraction or electrostatic pulsion play a role. These effects occur on a microscopic scale at the liquid–liquid interface and cannot be exactly quantified by measurement. Because of this, liquid–liquid phase separation cannot be described by simple correlations of characteristic quantities.

In order to characterize the settling behavior of a liquid–liquid dispersion, an experiment is required. We are using the batch-settling experiment because it is simple compared to others. In order to transfer the results of the batch-settling experiment to a settler operated in steady-state, it is necessary to derive a coalescence-specific parameter from the settling experiment that does not depend on the setup of the experiment. The estimation of such a parameter is shown in the following. The model considers drop sedimentation, balances of the amount of drops, drop deformation in the dense-packed zone and coalescence effects (drop–drop and drop–interface coalescences).

* Corresponding author. Tel.: +49-241-8095490; fax: +49-241-8092332.
E-mail address: secretary@tvt.rwth-aachen.de (A. Pfennig).

1385-8947/02/$ – see front matter
PII: S1385-8947(01)00251-0

Nomenclature

A_r	Archimedes number (–)
c_w	friction coefficient (–)
F	force (N)
g	acceleration due to gravity (m/s^2)
h	height (m)
H	Hamaker coefficient (N m)
K_{HR}	Hadamard–Rybczynski factor (–)
L	length (m)
La	Laplace number (–)
n	exponent (–)
o/w	volume ratio, organic to aqueous (–)
p	pressure (Pa)
q	defined by Eq. (6)
r	radius (m)
Re	Reynolds number (–)
t	time (s)
v	velocity (m/s)

Greek letters

ε	volume fraction of dispersed phase (–)
η	viscosity (Pa s)
ξ	defined by Eq. (4)
ρ	density (kg/m^3)
σ	interfacial tension (N/m)
τ	coalescence time (s)
Φ	Sauter diameter (m)
Δ	difference (–)

Subscripts

0	initial value (after mixing is stopped)
∞	in infinite extended fluid
a	out of contact area
c	continuous phase
d	dispersed phase
E	end
f	contact area
i	at the interface
p	dense-packed zone
py	running variable in the dense-packed zone
s	sedimentation
t	between two drops
v	asymmetrical
vdW	van der Waals
z	symmetrical

Superscripts

*	dimensionless
′	end of sedimentation
mod	modified

2. Description of drop sedimentation during the settling experiment

In the range of free sedimentation (i.e. drops have not entered the dense-packed zone yet), hardly any drop–drop coalescence takes place. Hence, the sedimentation curve in this range shows an almost linear slope (see Fig. 1). If the sedimentation velocity of the swarm of drops v_s is determined from the experimental sedimentation curve in the linear range, well known models reported in the literature can be applied to estimate the Sauter diameter of the drops. The sedimentation model for drop swarms reported by Pilhofer and Mewes [5] has been applied successfully:

$$Re_s = \frac{3q\varepsilon_0}{c_w\xi(1-\varepsilon_0)}\left[\left(1+Ar\frac{c_w\xi(1-\varepsilon_0)^3}{54q^2\varepsilon_0^2}\right)^{0.5}-1\right], \quad (1)$$

where

$$Re_s = \frac{\rho_c v_s \Phi_0}{\eta_c}, \quad (2)$$

$$Ar = \frac{\rho_c \Delta\rho g \Phi_0^3}{\eta_c^2}, \quad (3)$$

$$\xi = 5K_{HR}^{-3/2}\left(\frac{\varepsilon_0}{1-\varepsilon_0}\right)^{0.45}, \quad (4)$$

$$K_{HR} = \frac{3(\eta_c+\eta_d)}{2\eta_c+3\eta_d}, \quad (5)$$

$$q = \frac{1-\varepsilon_0}{2\varepsilon_0 K_{HR}}\exp\left(\frac{2.5\varepsilon_0}{1-0.61\varepsilon_0}\right), \quad (6)$$

$$c_w = \frac{Ar}{6Re_\infty^2} - \frac{3}{K_{HR}Re_\infty}. \quad (7)$$

This model is valid for Archimedes numbers above 1 and volume fractions of the dispersed phase (ε_0) between 0.06 and 0.55. The sedimentation of a single drop in an infinitely expanded fluid enters the model through the Reynolds number for particles Re_∞. In order to calculate Re_∞ in Eq. (7), Pilhofer and Mewes recommend a model given by Hu and Kintner [6]. However, this model is only valid for relatively large drops. For small droplets below roughly 1 mm diameter (depending on the system properties), the calculated sedimentation velocities can be negative. Because, in settling experiments, the range of drop sizes between 0.5 and 4 mm diameter is particularly important, the Hu and Kintner model cannot be applied. Comparing various other model equations, it turns out that smaller drops can be described using the equation given by Ishii and Zuber [7]:

$$Re_\infty = \frac{\rho_c v_{s,\infty}\Phi_0}{\eta_c} = 9.72[(1+0.01Ar)^{4/7}-1]. \quad (8)$$

Since with the equations given, it is possible to calculate the Sauter diameter from the sedimentation curve in the

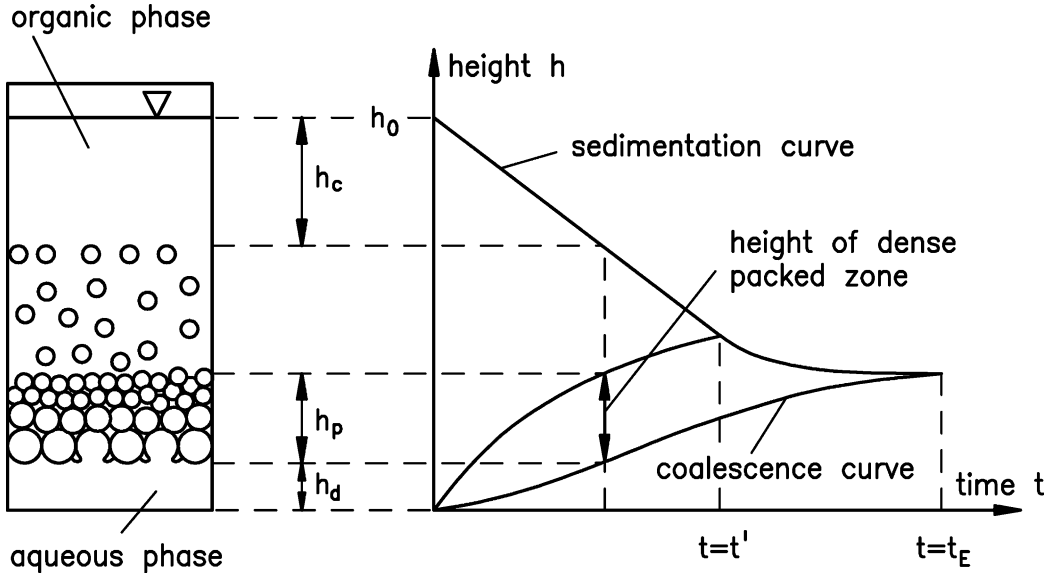

Fig. 1. Batch-settling experiment (left-hand side) and respective settling curve (right-hand side) with notation for different heights.

range of free sedimentation the difficult measurement of drop size during the settling experiment is not necessary. With the equations, the drop behavior between the sedimentation curve and the dense-packed zone (see Fig. 1) is described. Next, the height of the dense-packed zone will be calculated. For that some balances are necessary.

3. Balances

Fundamental research in this area was carried out by Hartland et al. [8,9]. Here, the important results which are necessary for the evaluation are summarized. A detailed derivation is presented elsewhere [8,9].

The slope of the coalescence curve, also referred to as coalescence velocity ($\mathrm{d}h_\mathrm{d}/\mathrm{d}t$) amounts to

$$\frac{\mathrm{d}h_\mathrm{d}}{\mathrm{d}t} = \frac{2\varepsilon_\mathrm{i}\Phi_\mathrm{i}}{3\tau_\mathrm{i}}. \tag{9}$$

Here ε_i ($\sim$1) is the hold up of the dispersed phase and Φ_i the Sauter diameter of the drops at the interface. τ_i represents the drop–interface coalescence time. Taking the drop–drop coalescence time τ_t into account, the drop growth in the dense-packed zone can be calculated from

$$\frac{\mathrm{d}\Phi(h,t)}{\mathrm{d}t} = \frac{\Phi(h,t)}{6\tau_\mathrm{t}}. \tag{10}$$

For $0 < t < t'$, the height of the dense-packed zone can be expressed by

$$h_\mathrm{p} = \frac{(h_0 - v_\mathrm{s}t)\varepsilon_0 - (1-\varepsilon_0)h_\mathrm{d}}{\varepsilon_{\mathrm{p},0} - \varepsilon_0}, \tag{11}$$

where

$$\varepsilon_{\mathrm{p},0} = \tfrac{1}{2}(\varepsilon_\mathrm{i} + \varepsilon_0) \tag{12}$$

represents the average volume fraction of the drops in the dense-packed zone. After free sedimentation is completed, the equation simplifies to

$$h_\mathrm{p} = \frac{h_0\varepsilon_0 - h_\mathrm{d}}{\varepsilon_\mathrm{p}}. \tag{13}$$

Since the sedimentation curve is continuous at $t = t'$, the hold up ε_p in the region $t \geq t'$ can be calculated by the following exponentially increasing expression:

$$\varepsilon_\mathrm{p} = \varepsilon_\mathrm{i} - \exp(-C_1 t - C_2) \tag{14}$$

with

$$C_1 = \left.\frac{(v_\mathrm{s} - \mathrm{d}h_\mathrm{d}/\mathrm{d}t)\varepsilon_{\mathrm{p},0}^2 + (\mathrm{d}h_\mathrm{d}/\mathrm{d}t)\varepsilon_{\mathrm{p},0}}{(h_\mathrm{d} - h_0\varepsilon_0)(\varepsilon_\mathrm{i} - \varepsilon_{\mathrm{p},0})}\right|_{t=t'}, \tag{15}$$

$$C_2 = -C_1 t' - \ln(\varepsilon_\mathrm{i} - \varepsilon_{\mathrm{p},0}). \tag{16}$$

The hold up at the interface is approximately unity. For the calculations, $\varepsilon_\mathrm{i} = 1$ is used.

In the above equations, the coalescence times τ_i and τ_t are still unknown. For the calculation of these times, the contact areas between a drop and the interface and between two drops are needed. Both contact areas depend on the drop deformation.

4. Drop deformation

For coalescence modeling, the drop geometry in the dense-packed zone is required. The higher the dense-packed zone, the stronger the deformation of the drops is due to the pressure exerted by the drops resting on them. As a consequence, the contact area (with radius r_f) between two drops increases and the radius r_a, which describes the contour

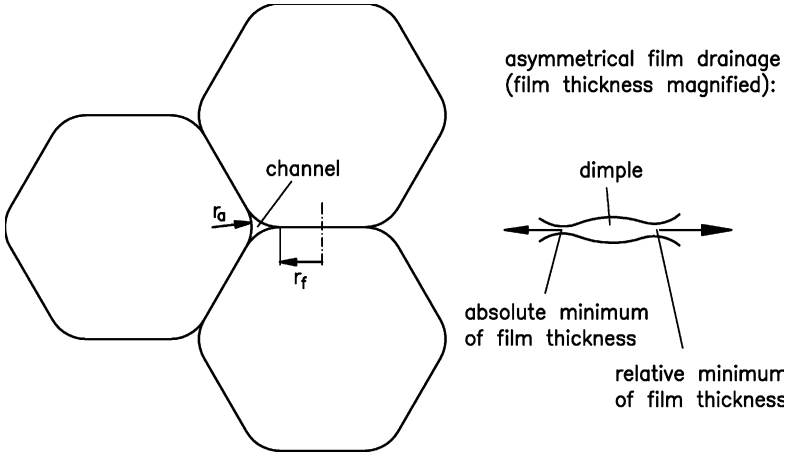

Fig. 2. Deformation of drops in the dense-packed zone (left side) and asymmetrical film drainage during coalescence process (right side).

of the channel formed between three drops, decreases (see Fig. 2). When drop deformation is very strong, the drops take a shape similar to that of a pentagonal dodecahedra [10].

The equations describing the drop deformation have to be solved numerically. Corresponding calculations were carried out. By close inspection of the calculated solutions, the following empirical formulae were derived by Henschke [11]:

$$r_{f,t} = 0.030\Phi\sqrt{1 - \frac{4.7}{4.7 + La}}, \tag{17}$$

$$r_a = 0.5\Phi\sqrt{1 - \frac{4.7}{4.7 + La}} \tag{18}$$

with

$$La = \frac{\Delta\rho g h_{py}\Phi}{\sigma}. \tag{19}$$

Here, La is the Laplace number which represents the ratio between the hydrostatic pressure and the interfacial tension. The hydrostatic pressure results from the drop-packing height h_{py} above the drop considered. Eq. (17) is valid for the contact area between two drops (index t) which is relevant for drop–drop coalescence. For drop–interface coalescence (index i), the contact area is about three times larger because, on account of the dodecahedral shape, approximately three pentagons are in contact with the interface. Therefore, the following approximation can be used:

$$r_{f,i} = r_{f,t}\sqrt{3}. \tag{20}$$

The derived equations for drop deformation are only valid under the following assumption: The channels between the drops are large enough to allow a free outflow of the continuous phase compressed between the drops. If this condition is not fulfilled, the drops are floated because they are pushed by the flow of the continuous phase against the direction of their sedimentation. Misek [12] and Jeelani et al. [13] also referred to this problem. As a matter of fact, the influence of the packing height is overestimated by far, if the drop deformation is calculated by the equations given above. Therefore, Henschke [11] modified the Laplace number, which is used in Eqs. (17) and (18) instead of that from Eq. (19):

$$La^{mod} = \left(\frac{\Delta\rho g}{\sigma}\right)^{0.6} h_{py}^{0.2}\Phi. \tag{21}$$

The exponents were fitted to the experimental data by comparing measured coalescence curves with the calculated ones. With the modified Laplace number, most of the experimental data are well described (see coalescence curves in Figs. 4–9).

5. Coalescence

For coalescence, the outflow of the fluid film between two drops or between a drop and its continuous phase is the time-determining factor.

In systematic investigations of the outflow [14–19], the film thickness h was recorded as a function of position and time. It was found that the thickness of the fluid film is not constant, but shows a minimum at the edge of the contact area instead. Furthermore, the fluid film is not rotationally symmetrical. This leads to an asymmetric film drainage relative to the normal axis of the contact area (see Fig. 2). Nice photographs that show the asymmetric film drainage in single drop experiments can be found, e.g. Fig. 1 in [14], Fig. 3 in [17] and Fig. 1 in [19]. From these experiments, it was found that the drops are the coalescing faster in the case of asymmetrical drainage than in the case of symmetrical drainage. Unfortunately in the literature, only the symmetrical case is considered in the mathematical models in detail. This leads to a dependence of the form

$$\tau \propto r_f^n, \tag{22}$$

in which n reaches from ~1.4 in [22,23] to over ~2 in [24,25] to 4.0 in [26,27]. However, if n is larger than unity,

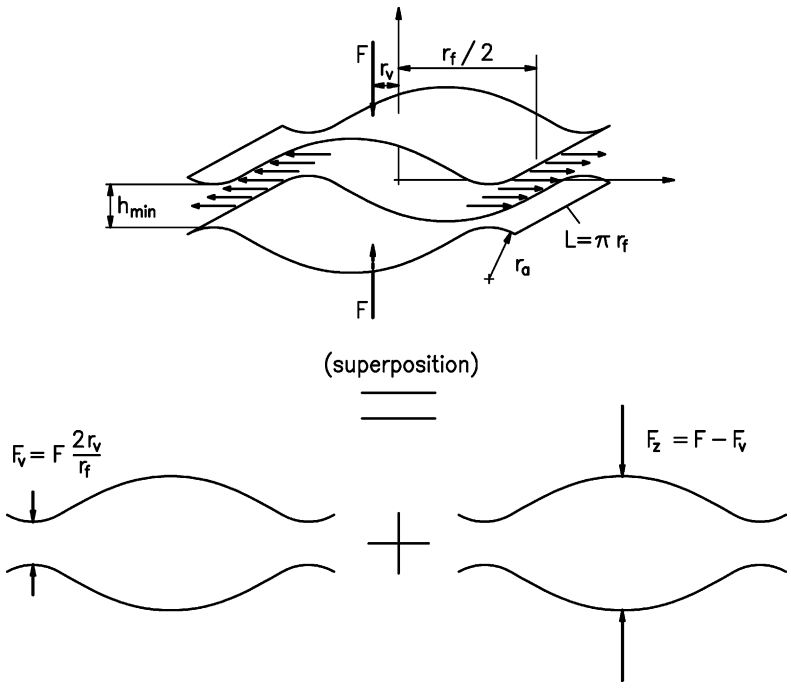

Fig. 3. Simplified model of the asymmetric film drainage.

the calculation of batch-settling results in an increasing decay time of the dense-packed zone with increasing drop diameter. This has never been observed in settling experiments.

If the no-slip condition (Stokes) is assumed at the interfaces, an asymmetric film drainage occurs when the resulting pressure force acting on the drainage film

$$F = \frac{\sigma}{r_a}\pi r_f^2 \tag{23}$$

is not located in the center of the film. For the modeling of the film drainage, let the displacement from the center be r_v and in dimensionless form

$$r_v^* = \frac{r_v}{r_f}. \tag{24}$$

The introduction of an asymmetric force may appear a little arbitrary since at least in the case of single drop experiments a symmetry along the vertical axis should exist. Nevertheless, the above mentioned photographs show an asymmetry in the drainage film. Local differences in the mobility of the interfaces are a possible explanation (Hartland [19]). Also Chesters [20] considers mobile interfaces in the modeling. If a mobile interface is the reason for the observed asymmetry, the displacement r_v^* can be interpreted as a virtual displacement. In this case, r_v^* is only a virtual aid for the modeling of asymmetrical film drainage.

In dense-packed dispersions, the conditions are very different compared to single drops. Just the density difference between the two phases results in an asymmetrical drainage if the film between two drops is not horizontal. Furthermore, there is a drop-size distribution in a dispersion. So not all drops have 12 neighbors and the drop deformation is not completely symmetrically as photographs show (see e.g. [21]). Since it is impossible to model all mentioned effects in detail, it seems adequate to summarize them in the parameter r_v^*.

In order to simplify the problem, a two-dimensional film is introduced as shown in Fig. 3. Since the bend of the film is small compared to its size, it is sufficient to consider the flow to be parallel to the horizontal coordinate. Applying the principle of superposition, the force F can be divided into a symmetric contribution F_z and an asymmetric contribution F_v. For the asymmetric contribution, the line of action is located exactly above the point of minimum film thickness. Dividing of the force leads to two flow problems which can be solved separately. The complete solution is obtained by superposition of both the solutions.

The approaching of the interfaces at the point of minimum film thickness, due to the symmetric force, can be estimated using an equation from Buevich and Lipkina [22]:

$$\frac{dh_{min}}{dt} = -0.812\frac{\sigma}{\eta_c r_a r_f^2}h_{min}^3. \tag{25}$$

The asymmetric force has two effects. On the side of its line of action (left side in Fig. 3), the interfaces approach each other quickly, whereas on the opposite side of the film, the film thickness increases due to the film fluid which is driven out of the dimple. Since the approaching of the interfaces is mainly determined by the flow in the narrowest region, the complex flow problem is reduced to the description of the approach of two cylinders with a radius r_a under the influence of the force F_v. If the approach suggested by McAvoy and Kintner [28] is chosen to design a model and the varied

geometry is taken into account (McAvoy and Kintner studied the approach of two spheres), the velocity of the approaching of the interfaces at the narrowest point can be expressed by

$$\frac{\mathrm{d}h_{\min}}{\mathrm{d}t} = -\frac{2F_{\mathrm{v}}}{3\pi\eta_{\mathrm{c}}L}\left(\frac{h_{\min}}{r_{\mathrm{a}}}\right)^{3/2}. \tag{26}$$

Substituting F_{v} (see Eqs. (23) and (24), Fig. 3) and L (see Fig. 3) leads to the velocity of approaching of the interfaces:

$$\frac{\mathrm{d}h_{\min}}{\mathrm{d}t} = -\frac{4\sigma r_{\mathrm{f}} r_{\mathrm{v}}^{*}}{3\pi\eta_{\mathrm{c}} r_{\mathrm{a}}^{5/2}} h_{\min}. \tag{27}$$

This velocity and the velocity given by Eq. (25) have to be superimposed to obtain the total velocity of approaching of the interfaces. In practice, however, $\mathrm{d}h_{\min}/\mathrm{d}t$ caused by the symmetric force component is considerably smaller than that due to the asymmetric component. In this case, the coalescence time can be obtained by the integration of Eq. (25) with the integration limits of $h_{\min} = \infty, \ldots, h$ and $t = 0, \ldots, \tau$:

$$\tau = -\frac{3\pi\eta_{\mathrm{c}} r_{\mathrm{a}}^{5/2}}{2\sigma r_{\mathrm{f}} r_{\mathrm{v}}^{*} h^{1/2}}. \tag{28}$$

After the interfaces have approached each other in such a way that the van der Waals attraction [29]

$$p_{\mathrm{vdW}} = \frac{H}{6\pi h^{3}} \tag{29}$$

is of the same order of magnitude as the internal drop pressure $p_{\mathrm{f}} = \sigma/r_{\mathrm{a}}$, the interfacial tension can no longer maintain the cylindrical shape of the interfaces. Consequently, the drops coalesce (see also figures in [30,31]).

Inserting the thickness h, which can be obtained from $p_{\mathrm{f}} = p_{\mathrm{vdW}}$, into Eq. (28) leads to

$$\tau = \frac{(6\pi)^{7/6}\eta_{\mathrm{c}} r_{\mathrm{a}}^{7/3}}{4\sigma^{5/6} H^{1/6} r_{\mathrm{f}} r_{\mathrm{v}}^{*}}. \tag{30}$$

This equation contains two unknown parameters: the Hamaker coefficient H and the asymmetry parameter r_{v}^{*}. The asymmetry parameter is adjusted to experimental settling curves and thus is characteristic for the system used. The Hamaker coefficient generally can be determined experimentally, but the values found in the literature for a specific system can vary by a factor of 10. On the other hand, for many systems, the Hamaker coefficient lies within the same order of magnitude [32]. Since the Hamaker coefficient hardly affects the coalescence time due to the exponent 1/6 in Eq. (30), and because additionally, errors concerning the Hamaker coefficient are compensated by the fit of the asymmetry parameter, its value is fixed here to 1×10^{-20} N m for all systems.

The settling experiment is completely described by Eqs. (1)–(21) and (30). Their solution, i.e. the calculation of settling curves, can only be obtained numerically. For this purpose, an algorithm was developed which consists of two nested loops. The outer loop runs over discrete time intervals Δt while in the inner loop discrete height elements Δh_{p} are considered. In the inner loop, the drop growth in Δt due to drop–drop coalescence in the dense-packed zone and the drop–interface coalescence is calculated.

6. Results and discussion

Siemons [33] carried out settling experiments in a stirred cylindrical vessel with a filling height of 400 mm. He determined the Sauter diameter of the drops in the dispersion at several heights as a function of time. The results for the system cyclohexanone/water are shown in Fig. 4. The Sauter diameters are shown as scaled circles.

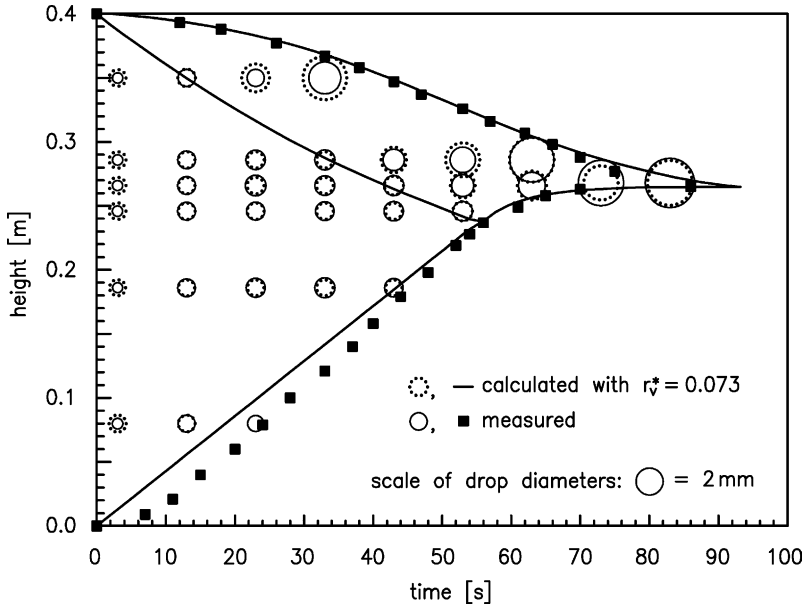

Fig. 4. Drop growth inside the dispersion during the settling process. Experimental data of Siemons [33]: cyclohexanone dispersed in water, o/w=1/2.

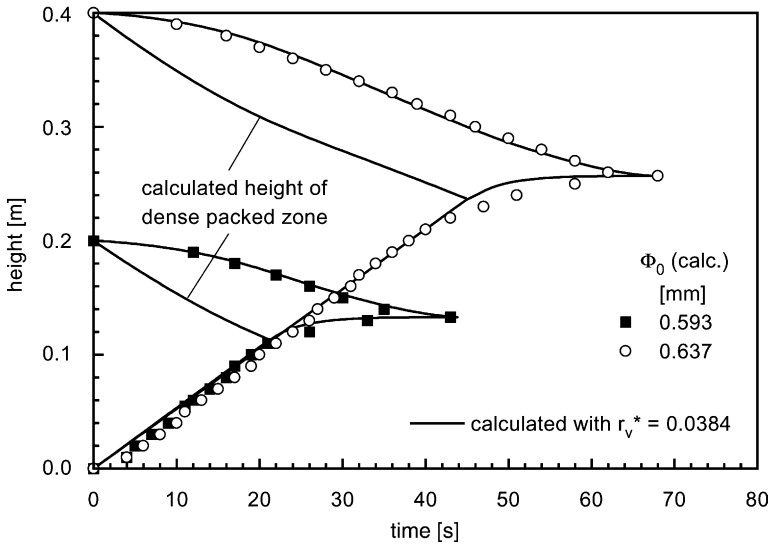

Fig. 5. Influence of the filling height on the settling curve during the settling experiment. Experimental data of Siemons [33]: methyl-isobutyl ketone dispersed in water, o/w=1/2.

In contrast to Fig. 1 here, the light phase is dispersed in the heavy phase. However, this means no principal difference in the modeling.

A significant increase of the Sauter diameter can be observed in the decreasing turbulence field during approximately the first 13 s after mixing has been stopped. After that (13–53 s), the Sauter diameter in the region of free sedimentation does not change any more and is well described by the model.

Inside the dense-packed zone, the Sauter diameter increases as time proceeds. The drops coalescing at the end of the settling process due to drop–interface coalescence are more than three times larger than the drops initially generated. Both, the growth of the drops as well as the slope of the coalescence curve, are satisfactorily described by the model. It is worth noting that the calculated drop diameters in the dense-packed zone are not adjusted to the experimental data but are truly predicted. Only the asymmetry parameter of the coalescence model (r_v^* in Eq. (30)) was adjusted to the experimental data of the coalescence curve. In this case, r_v^* turned out to be 0.073.

In another series of measurements, Siemons varied the filling height in the settling cylinder. The settling curves obtained for the system methyl-isobutyl ketone (MiBK)/water are shown in Fig. 5 for filling heights of 400 and 200 mm, respectively (symbols) together with the calculated settling curves (full lines). For both filling heights, the settling curves can be well described with the same value (0.0384) of the asymmetry parameter.

Fig. 6 shows the experimental data of Nadiv and Semiat [34]. They used a mixture of *n*-heptane + paraffin oil which was dispersed in water. The settler diameter was 65 mm and the initial dispersion height was varied from 315 to 945 mm. The full lines are calculated with the proposed model using $r_v^* = 0.0053$. Although the model estimates the decay time for the smallest height a little large, the agreement is acceptable.

The dispersion is usually produced by an impeller. So it is to be expected that the drop size depends on the agitation speed. Indeed in the literature (summary in [35]), a corresponding dependence is reported. On the other hand, a change in the drop diameter could only be observed rarely in the settling experiments when the agitation speed was varied while the other conditions were kept constant. This discrepancy is probably due to the considerable drop–drop coalescence during the first few seconds of the settling process (see Fig. 4).

One example where a dependence of the settling curves and thus of the drop size on the intensity of mixing was observed is shown in Fig. 7. The measurements were carried out by Berger [36]. The figure shows three settling curves of the liquid–liquid system, cyclohexane/water. The agitation speed was 300, 450 and 600 rpm, respectively. The calculation of the three curves with the model introduced above gives a Sauter diameter of 1.027 mm for the fastest phase separation. For the other curves, $\Phi_0\,(\text{calc}) = 0.606$ and 0.488 mm are obtained. All the three settling curves can be described with the identical r_v^*=0.0297. If each of the curves is fitted separately, values of 0.0299, 0.0290 and 0.0302 result (the quickest to the slowest phase separation). Thus r_v^* can be determined clearly with high significance from a single settling curve and does not depend on the drop diameter.

The variation of the phase ratio usually leads to a change of the drop diameter in the settling experiments because typically at low values of the hold up small drops are generated during the dispersion process. In Fig. 8, settling curves for different phase ratios are shown. The experiments were carried out by Henschke [11] in a stirring vessel

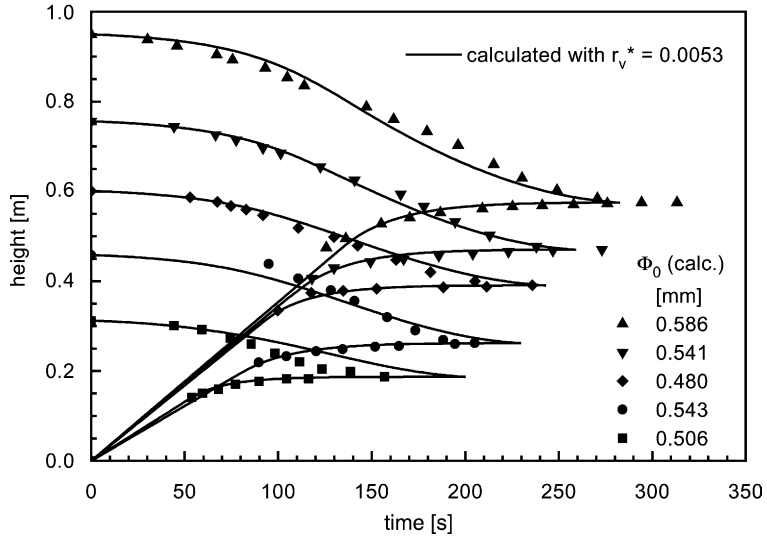

Fig. 6. Influence of the filling height on the settling curve during the settling experiment. Experimental data of Nadiv and Semiat [34]: mixture of heptane and paraffin oil dispersed in water, o/w=2/3, settler diameter = 65 mm.

containing two counter-rotating shafts. With this setup, a vortex is avoided without using inserts that might influence coalescence.

For both o in w dispersions and w in o dispersions (shown in Fig. 8), the smallest Sauter diameter calculated from the sedimentation curve (0.612 and 0.530, respectively) results from the smallest volume fraction of the dispersed phase (o/w = 1/4 and o/w = 4/1, respectively). Furthermore, not only the drop diameter but also the velocity of interfacial coalescence decreases with decreasing volume fraction of the dispersed phase. The dependency between volume fraction, sedimentation rate and coalescence rate is well described with a constant value of r_v^*. Fitting of the experimental settling curves yields $r_v^* = 0.0383$ for the o in w experiments and 0.0385 for the w in o experiments. Even though these values are almost identical in this special case, it cannot be concluded that this is always so. In most cases, the value of this parameter changes significantly if the type of the dispersion is changed.

Concerning experiments with varying volume fraction, it has to be noted that the mutual saturation of the phases (before they are filled in the stirring vessel) happens at a constant phase ratio. By this procedure, the amount of trace impurities which are extracted from one phase into the other is constant. Only if this is ensured, different phase ratios can be characterized by a constant parameter r_v^*.

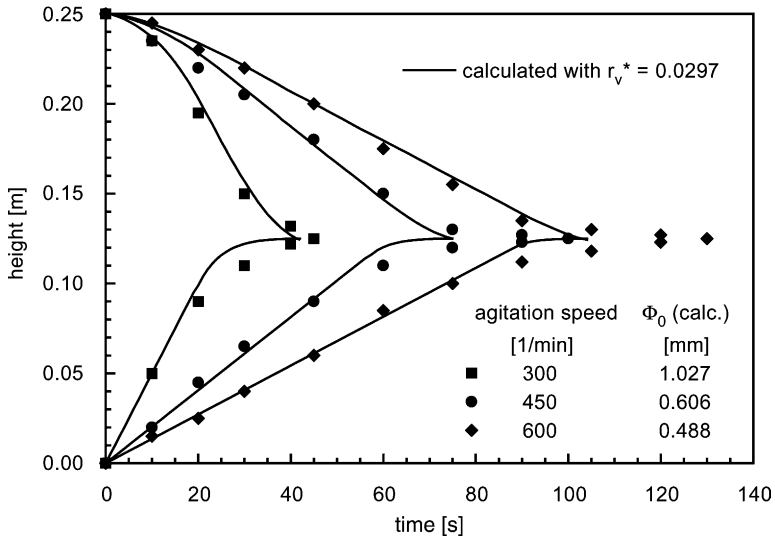

Fig. 7. Influence of the mixing speed on phase separation. Experimental data of Berger [36]: cyclohexane dispersed in water, o/w=1/1, settler diameter = 38 mm.

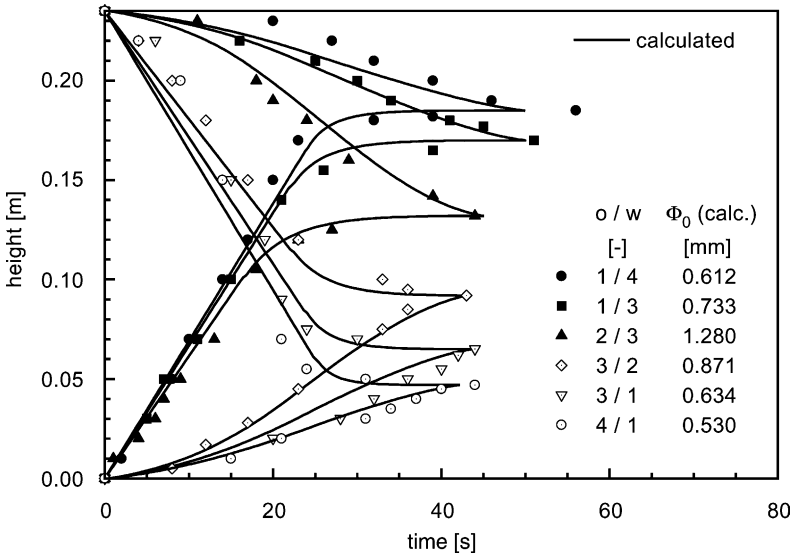

Fig. 8. Influence of the phase ratio on phase separation. Experimental data of Henschke [11]: *n*-butyl acetate/water; filled symbols, o dispersed in w (r_v^*= 0.0383); open symbols, w dispersed in o (r_v^*= 0.0385); settler diameter = 80 mm.

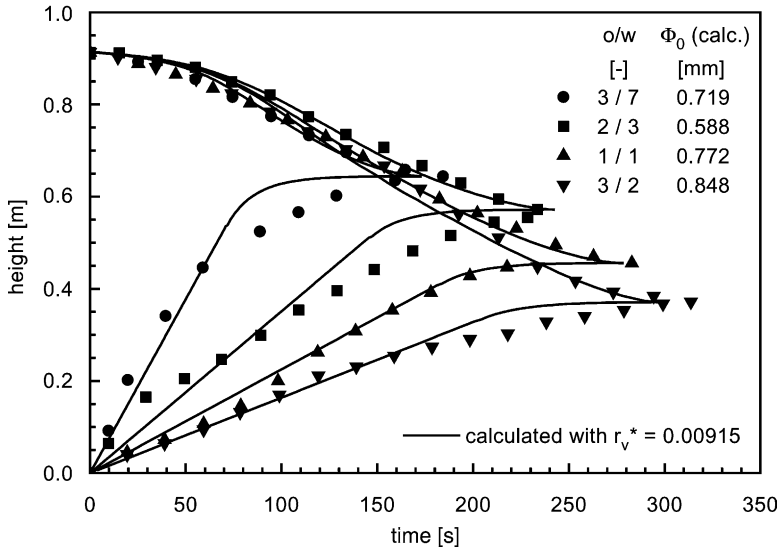

Fig. 9. Influence of the phase ratio on phase separation. Experimental data of Jeelani and Hartland [37]: mixture of 25 vol.% decane and 75 vol.% paraffin oil dispersed in water, settler diameter = 25 mm.

In the experiments of Henschke [11], the sedimentation rate is almost independent of the phase ratio but the coalescence rate varies. A different behavior was observed by Jeelani and Hartland [37]. In their experiments with different phase ratios, the coalescence rate varies and the sedimentation rate is almost constant. Probably this is an effect of the solvent used (*n*-butyl acetate and decane + paraffin oil mixture, respectively). The model proposed here is also capable of describing this effect. The evaluation of the data of Jeelani and Hartland results in $r_v^* = 0.00915$ for all the phase ratios. The experimental data are shown together with model calculations in Fig. 9.

7. Conclusion

The parameter r_v^* calculated from only one settling curve is independent of the filling height in the vessel (Figs. 5 and 6), the mixing intensity (Fig. 7) and the volume fraction of the dispersed phase (Figs. 8 and 9).

This behavior indicates that r_v^* is a basic parameter which characterizes the properties of coalescence of a liquid–liquid system. Furthermore, the model is able to describe the increase in drop size in the dense-packed zone without an additional parameter (Fig. 4).

If mass transfer occurs during the settling process as investigated, e.g. by Kyuchoukov and Kounev [38], a limit of

the model is reached. In this case, Marangoni effects have to be taken into account in the hydrodynamic modeling.

References

[1] R. Berger, Koaleszenzprobleme in chemischen Prozessen, Chem. Ing. Technol. 58 (1986) 449–456.
[2] K.-H. Reissinger, J. Schröter, W. Becker, Möglichkeiten und Probleme bei der Auslegung von Extraktoren, Chem. Ing. Technol. 53 (1981) 607–614.
[3] M. Stönner, F. Wöhler, An engineer's approach to a solvent extraction problem, IChemE Symp. Ser. 42 (1975) 14.1–14.12.
[4] E. Blaß, W. Meon, W. Rommel, A. Löbmann, Is hydrodynamic modeling a sound approach for the design of gravity settlers without coalescing aids? Int. Chem. Eng. 32 (4) (1992) 601–618.
[5] Th. Pilhofer, D. Mewes, Siebboden—Extraktionskolonnen, Verlag, Weinheim, 1979.
[6] S. Hu, R.L. Kintner, The fall of single liquid drops through water, AIChE J. 1 (1955) 42–48.
[7] M. Ishii, N. Zuber, Drag coefficient and relative velocity in bubbly, droplet or particulate flows, AIChE J. 25 (5) (1979) 843–855.
[8] S. Hartland, S.A.K. Jeelani, Prediction of sedimentation and coalescence profiles in a decaying batch dispersion, Chem. Eng. Sci. 43 (9) (1988) 2421–2429.
[9] S. Hartland, D.K. Vohra, Koaleszenz in vertikalen dichtgepackten dispersionen, Chem. Ing. Technol. 50 (9) (1978) 673–682.
[10] A.M.A. Allak, G.V. Jeffreys, Studies of coalescence and phase separation in thick dispersion bands, AIChE J. 20 (3) (1974) 564–570.
[11] M. Henschke, Dimensionierung liegender Flüssig–flüssig Abscheider anhand diskontinuierlicher Absetzversuche, Fortschritt-Berichte VDI, Reihe 3, Nr. 379, VDI-Verlag, Düsseldorf, 1995.
[12] T. Misek, The components of the coalescence process in dense dispersions, Proc. ISEC'86 III (1986) 71–79.
[13] S.A.K. Jeelani, K. Panoussopoulos, S. Hartland, Effect of turbulence on the separation of liquid–liquid dispersions in batch settlers of different geometries, Ind. Eng. Chem. Res. 38 (1999) 493–501.
[14] K.A. Burrill, D.R. Woods, Film shapes for deformable drops at liquid–liquid interfaces. II. The mechanisms of film drainage, J. Colloid Interf. Sci. 42 (1) (1973) 15–34.
[15] K.A. Burrill, D.R. Woods, Film shapes for deformable drops at liquid–liquid interfaces. III. Drop rest-times, J. Colloid Interf. Sci. 42 (1) (1973) 35–51.
[16] S. Hartland, The coalescence of a liquid drop at a liquid–liquid interface. Part I: Drop shape, Trans. Instn. Chem. Engrs. 45 (1967) 97–101.
[17] S. Hartland, The coalescence of a liquid drop at a liquid–liquid interface. Part II: Film thickness, Trans. Instn. Chem. Engrs. 45 (1967) 102–108.
[18] S. Hartland, The coalescence of a liquid drop at a liquid–liquid interface. Part III: Film rupture, Trans. Instn. Chem. Engrs. 45 (1967) 109–114.
[19] S. Hartland, The effect of circulation patterns on the drainage of the film between a liquid drop and a deformable liquid–liquid interface, Chem. Eng. Sci. 24 (1969) 611–613.
[20] A.K. Chesters, The modelling of coalescence processes in fluid–liquid dispersions: a review of current understanding, Trans. IChemE A 69 (1991) 259–270.
[21] S. Hartland, Koaleszenz in dichtgepackten Gas/Flüssig- und Flüssig/Flüssig-Dispersionen, Ber. Bunsenges. Phys. Chem. 85 (1981) 851–863.
[22] Y.A. Buevich, E.K. Lipkina, Disruption of thin liquid films, Colloid J. USSR (Engl. Trans.) 40 (2) (1978) 167–171.
[23] J.-D. Chen, A model of coalescence between two equal-sized spherical drops or bubbles, J. Colloid Interf. Sci. 107 (1) (1985) 209–220.
[24] L. Dongming, Coalescence between small bubbles: effects of bulk and surface diffusion, Chem. Eng. Sci. 51 (14) (1996) 3623–3630.
[25] L. Dongming, Coalescence between small bubbles: effects of surface tension gradient and surface viscosities, J. Colloid Interf. Sci. 181 (1996) 34–44.
[26] S. Hartland, Coalescence in dense-packed gas/liquid and liquid/liquid dispersions, Tenside Det. 18 (1981) 178–189.
[27] G.E. Charles, S.G. Mason, The coalescence of liquid drops with flat liquid/liquid interfaces, J. Colloid Sci. 15 (1960) 236–267.
[28] R.M. McAvoy, R.C. Kintner, Approach of two identical rigid spheres in a liquid field, J. Colloid Sci. 20 (1965) 191–204.
[29] H.C. Hamaker, The London–van der Waals attraction between spherical particles, Physica IV (10) (1937) 1058–1072.
[30] P.S. Hahn, J.D. Chen, J.C. Slattery, Effects of London–van der Waals forces on the thinning and rupture of a dimpled liquid film as a small drop or bubble approaches a fluid–fluid interface, AIChE J. 31 (12) (1985) 2026–2038.
[31] J. Eggers, J.R. Lister, H.A. Stone, Coalescence of liquid drops, J. Fluid Mech. 401 (1999) 293–310.
[32] J. Visser, On Hamaker constants: a comparison between Hamaker constants and Lifshitz–van der Waals constants, Adv. Colloid Interf. Sci. 3 (1972) 331–363.
[33] N. Siemons, Untersuchung zur Dimensionierung von Flüssig–flüssig–Abscheidern ohne Einbauten, Ph.D. Thesis, RWTH Aachen, 1985.
[34] C. Nadiv, R. Semiat, Batch settling of liquid–liquid dispersion, Ind. Eng. Chem. Res. 34 (1995) 2427–2435.
[35] C.A. Coulaloglou, L.L. Tavlarides, Drop size distributions and coalescence frequencies of liquid–liquid dispersions in flow vessels, AIChE J. 22 (2) (1976) 289–296.
[36] R. Berger, Einflüsse auf das Verhalten bei der Phasentrennung von nichtlöslichen Systemen organisch-wässrig, Presented at the Verfahrenstechnisches Kolloquium, RWTH Aachen, 1987.
[37] S.A.K. Jeelani, S. Hartland, Effect of dispersion properties on the separation of batch liquid–liquid dispersions, Ind. Eng. Chem. Res. 37 (1998) 547–554.
[38] G. Kyuchoukov, R. Kounev, On the coalescence effects in a batch mixer–settler, Chem. Eng. J. 69 (1998) 63–67.